EngOpt 2008 - International Conference on Engineering Optimization
Rio de Janeiro, Brazil, 01 - 05 June 2008.

Mixed-variable optimal design of induction motors including efficiency, noise and thermal criteria

J. Le Besnerais[1], A. Fasquelle[1,2], V. Lanfranchi[3], M. Hecquet[1], and P. Brochet[1]

[1]Laboratoire d'Electrotechnique et d'Electronique de Puissance (L2EP), Ecole Centrale de Lille, Cité Scientifique, 59651 Villeneuve d'Ascq, FRANCE (e-mail:jean.le_besnerais@centraliens.net)
[2]Laboratoire de Mécanique et d'Energétique (LME), Universit de Valenciennces, Le Mont Houy, 59313 Valenciennes, FRANCE (e-mail: aurelie.fasquelle@ec-lille.fr)
[3]Laboratoire d'Electromécanique de Compiègne (LEC), Université de Technologie de Compiègne, 60200 Compiègne, FRANCE (e-mail: vincent.lanfranchi@utc.fr)

1. Abstract

Squirrel cage induction motors design requires making numerous trade-offs, especially between its audible electromagnetic noise level, its efficiency and its material cost. However, adding the vibro-acoustic and thermal models to the usual electrical model of the motor drastically increases the simulation time. A finite element approach is then inconceivable, especially if the model has to be coupled to an evolutionary optimization algorithm.

A fast simulation tool of the variable-speed induction machine, based on electrical, mechanical, acoustic and thermal analytical models, has therefore been elaborated. It has been validated at different stages with both tests and finite element method (FEM) simulations. This model is then coupled to a mixed-variable constrained Non-dominating Sorting Genetic Algorithm (NSGA-II) with a stochastic repair algorithm. Some global optimizations with respect to several objectives (noise level, efficiency and material cost), including thermal constraints, are finally presented, and several convenient visualizations of multi-dimensional solutions are presented.

2. Keywords: Multi-objective optimization, multi-physics modelling, induction machine, thermal nodal network, acoustic noise.

3. Introduction

Squirrel-cage induction machines are widely used in the industry for their easy manufacturing and robustness. For instance, variable-speed induction motors are particularly present in electrical transport systems such as subways and trains. Their design variables are principally sized by the constraint to produce a given torque at a given speed, with the highest efficiency and, of course, fulfilling some mechanical and thermal constraints. A proper motor cooling is essential for subways, as they are continuously subjected to starting and breaking cycles.

With the climbing raw materials market, material cost has become another influential factor on the design process besides torque, temperature and efficiency. The environmental impact of the motor is also gaining increasing attention: in addition to the minimization of electricity consumption, the acoustic comfort of train passengers and frontage residents has to be ensured. While the aerodynamic sources of noise (fans) can be reduced by reducing the motor temperature, the magnetic noise issue, mainly due to Maxwell air-gap forces which make the stator vibrate in the audible range [1, 2, 3], has to be tackled in a different way.

The problem of induction motor optimal design has received much attention since the beginning of computer science [4, 5, 6, 7, 8]. Indeed, many trade-offs have to be made: for example, a smaller air-gap improves the efficiency, but increases the magnetic sound power level ; increasing the stator height of yoke to diameter ratio generally lowers magnetic vibrations [9], but it heightens material cost, and with a fixed motor size, it decreases the available output torque and highers rotor temperature [8]. Nevertheless, dealing with both noise and thermal criteria in an induction motor optimal design process has never been done.

When treating several conflicting objectives, using Pareto-optimality-based algorithms like the recent Non-dominated Sorting Genetic Algorithm (NSGA-II) [10] is notably fitted to the industrial framework:

they do not reach a single optimal solution, but determine a large set of Pareto-optimal solutions (the so-called Pareto front). Thus, a degree of freedom is still available at the end of optimization process, and final solutions can be evaluated with additional criteria or engineer know-how that are not included in the models (e.g. mechanical stress aspects). In addition, noise radiation highly depends on the number of stator and rotor teeth, which are discrete variables: besides constraints and several objectives, the optimization algorithm must therefore also handle mixed-variable.

As genetic algorithm are quite greedy, the use of coupled electrical, mechanical, acoustical and thermal FEM simulations to evaluate the objective functions is inconceivable, even more when these simulations have to be carried at several speeds in order to account for resonance effects. A fully analytical model, DIVA, has been therefore developed and validated with tests and FEM.

Firstly, this article presents this multi-disciplinary analytical model, with an emphasis on the nodal-network based thermal model. Then, the optimization problem is defined, and the NSGA-II method is presented. Some optimization results are finally detailed, and analysed by the aid of several convenient visualizations of the multi-dimensional Pareto-optimal solutions.

4. Electromagnetic, thermal, mechanical and acoustic models

4.1. Electromagnetic model

Stator current computation is based on a fundamental single phase equivalent circuit of the machine, where saturation effect is considered computing a saturation factor [11]. Stator currents have been validated with tests at several supply frequencies and saturation levels (Fig. 1).

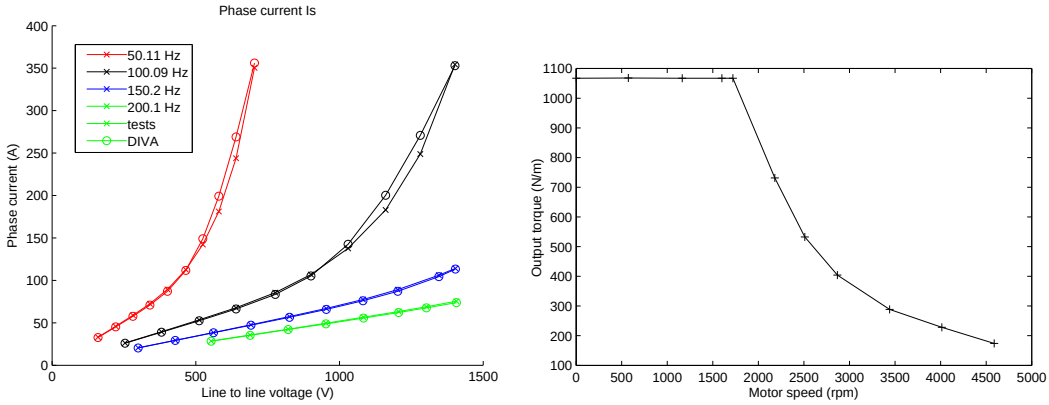

Figure 1: Left: comparison between test and simulated stator phase currents at several supply frequencies and supply voltages. Right: specified output torque in function of motor speed during starting phase (the nominal speed, at which the motor run the most, is here 2200 rpm).

The air-gap radial flux-density distribution, which is used in order to compute the magnetic force distribution acting on stator core, is computed as the product of magnetomotive force and air-gap permeance. It has been validated with the FEM software FLUX2D [12].

During variable-speed simulations, a torque/speed curve is specified (Fig. 1). Fundamental supply voltage and slip are then calculated by iteratively solving the equivalent circuit in order to reach the aimed output torque. Fundamental torque computation has been validated by tests and FEM [12].

Motor efficiency η is computed as

$$\eta = \frac{P_{out}}{P_{in}} = \frac{P_{mec} - P_{ir}^{R}}{P_{em} + P_{ir}^{SC} + P_{ir}^{ST} + P_{j}^{S}} \tag{1}$$

where P_{mec} is the mechanical air-gap power, P_{em} is the air-gap electromagnetic power, P_{ir}^{R} represents rotor total iron losses, P_{ir}^{SC} and P_{ir}^{ST} stator core and teeth iron losses, and P_{j}^{S} stator Joule power losses.

4.2. Thermal model

A 3D nodal network-based thermal model is used in order to compute stator and rotor mean temperature in steady state. This method consists in dividing the machine in small isotherm volumes whose centre is represented by nodes. Each node is then associated to a volume V_i, a temperature T_i, a heat capacity C_i, and a heat sink/source P_i. By analysing the types of heat transfers (convective, diffusive, etc) that occurring the different parts of the machine, nodes can be connected one to another with equivalent thermal conductances G_{ij}. The evolution of nodes temperature can then be modelled by the equation

$$\mathbf{C}\frac{d\mathbf{T}}{dt} = \mathbf{G}\mathbf{T} - \mathbf{G}_{bc}(\mathbf{T} - T_a) + \mathbf{P} \tag{2}$$

where $\mathbf{T}$ is the vector of nodes temperature, $\mathbf{C}$ is the diagonal matrix of capacities, $\mathbf{G}$ is the conductances matrix, $\mathbf{G}_{bc}$ is the conductances matrix corresponding to boundary conditions (T_a being the ambient temperature outside the motor), and $\mathbf{P}$ is the vector of heat sources. The solution of this equation $\mathbf{T}_f$ in steady state is given by

$$\mathbf{T}_f = -(\mathbf{G} - \mathbf{G}_{bc})^{-1}(\mathbf{P} + \mathbf{G}_{bc}T_a) \tag{3}$$

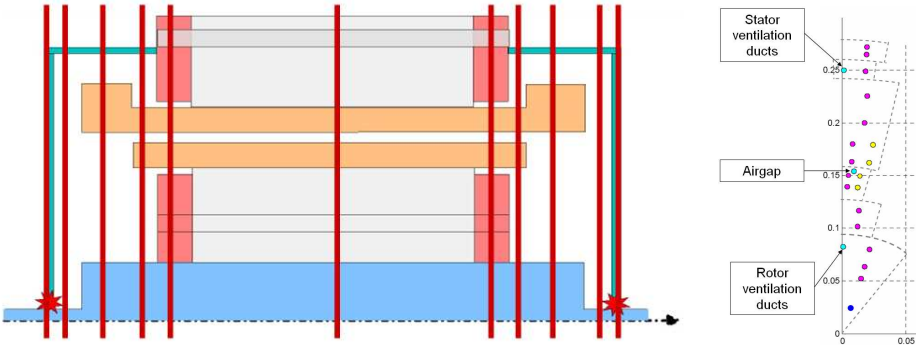

Figure 2: Left: representation of the 11 nodal network layers in a half motor. Right: representation of the middle layer nodes.

The nodal network has a total number of 126 nodes allocated to 11 different layers in the axial direction of the motor (Fig. 2).

Heat sources are due to Joule losses, iron losses and friction losses. Joule losses and iron losses are computed using the electromagnetic model: iron losses are modelled with a Steinmetz formula, where different coefficients are used for stator yoke, stator teeth and rotor regions [13] and were fit to finite element simulations. Friction losses account for aerodynamic friction in the air-gap, and mechanical friction due to bearings. Aerodynamic and bearings frictions are computed as polynomial functions of motor speed, which were fitted to experiments. Convective heat transfer coefficients have been also expressed as polynomial functions of speed, and fitted with finite volume numerical simulations [14].

4.3. Mechanical model

Neglecting the tangential component of the Maxwell tensor and magnetostrictive effect, the radial exciting pressure P_M which is supposed to be responsible for magnetic noise can be approximated by

$$P_M = B_g^2/(2\mu_0) \tag{4}$$

Dynamic deflections $Y^d_{m\omega}$ of stator structure are then computed from the 2D discrete Fourier transform $P_{m\omega}$ of P_M [15, 1, 2, 9]. Natural frequencies f_m are computed assimilating the stator as a 2D ring. Natural frequencies computation has been validated with FEM and experiments [16, 9, 17].

4.4. Acoustic model

The sound powers $W_m(f)$ radiated by the vibrations of order m and frequency f are first computed as a function of $v_{m\omega}$. The sound power level $L_w(f)$ is then obtained as

$$L_w(f) = 10\log_{10}\left(\sum_m W_m(f)/W_0\right), \quad W_0 = 10^{-12}\text{W} \tag{5}$$

Total A-weighted sound power level L_{wA} is computed summing sound powers $L_w(f)$ weighted with human ear sensitivity at frequency f. The acoustic model was favourably compared to noise measurements made on a water-cooled induction machine [18]. More details about this analytical model can be found in [9].

5. Optimization problem

5.1. Definition

If $\mathbf{f} = (f_1, ..., f_M)$ is the vector of objective functions to minimize, where f_i functions depend on the design variables vector $\mathbf{X} = (X_1, ..., X_D)$, the corresponding constrained optimization problem can be written as

$$\begin{cases} \min \mathbf{f}(\mathbf{X}) \\ \textit{subject to} \quad \mathbf{G}(\mathbf{X}) \leq 0 \end{cases} \tag{6}$$

where $\mathbf{G}$ is the inequality constraints vector.

5.2. Objective functions

As explained in the introduction, the three objective functions that are considered are magnetic noise level, efficiency η, and material cost M_c. M_c is determined by computing the motor iron, aluminum and copper masses, and their corresponding market cost. Efficiency is maximized by minimizing $1/\eta$. The specified torque in function of speed is treated as a constraint, as well as temperature. However, two noise objective functions are computed in order to decrease both the maximum noise level encountered during traction phase, L_w^M, and the average noise level, L_w^m [19]. Contrary to material cost, efficiency depends on motor speed, and is therefore computed at nominal speed. The objective functions vector has thus 4 components.

5.3. Design variables

The electromagnetic, thermal, mechanical and acoustic models involve more than a hundred variables, but the most influential ones on the target functions have been already identified using a sensitivity analysis tool [12].

The design variables optimized in this article are listed in Table 1. They represent rotor and stator slot shapes, as well as stator diameter and height of yoke, and rotor teeth number which has a strong influence on noise. The problem therefore involves both continuous and discrete variables. The discrete variable of stator teeth number is not varied because of an industrial constraint. However, an optimization problem involving Z_s has already been treated in a previous work [20].

The other design variables that are not modified during optimization are fixed according to a known industrial design $\mathbf{X}_{ref}$ with p=2 pole-pairs and Z_s=36 rotor slots.

5.4. Constraints

Besides 19 geometrical inequality constraints, the upper limits on flux densities in teeth and yokes are fixed, as well as the maximum saturation factor, and the upper limits on rotor and stator mean

Table 1: Description of the optimization problem design variables. Other variables are fixed according to a given industrial design.

Name	Description	Range	Type (C:continuous, D:discrete)
D_s	stator core diameter	[300, 700] mm	C
h_s	stator height of yoke	[32, 74] mm	C
w_{ss}	stator slot opening width	[6, 14] mm	C
$B3$	stator slot base width	[8, 16] mm	C
$H3$	stator slot depth	[23, 44] mm	C
g	air-gap width	[0.9, 2.1] mm	C
w_{rs}	rotor slot opening width	[2, 4.7] mm	C
$B5$	rotor slot small basis	[5.9, 10.6] mm	C
$B6$	rotor slot large basis	[9.5, 17.2] mm	C
$H5$	rotor slot depth	[17, 32] mm	C
$H4$	rotor isthmus width	[2.4, 7] mm	C
D_{sh}	rotor shaft diameter	[60, 140] mm	C
Z_r	rotor teeth number	$\{2k; k \in [10..40]\}$	D

temperature in steady state. The inequality constraints vector $\mathbf{G}$ has therefore 24 elements. When specified torque cannot be achieved by an individual, a penalization technique is used and its objectives are forced to a high value. The total external diameter of the motor, including frame, is limited.

5.5. Resolution

5.5.1 Optimization method

Induction motor optimal design is therefore a mixed-variable constrained multi-objective optimization problem. Several optimization algorithms can treat that kind of problem [21], but the recent multi-objective evolutionary algorithm NSGA-II has been here chosen for its easiness to handle constraints and mixed-variables. The implementation of these two features are detailed for instance in [20]. NSGA-II algorithm uses an elitist approach [10, 22], and relies on two main notions: non-domination relation, and crowding distance. Non-domination ranking is a way to sort individuals when considering more than one objective to minimize, whereas crowding distance is a criterion ensuring that optimal solutions are uniformly spread in objectives space. Details on this algorithm can be found in [10].

5.5.1 Stochastic repair algorithm

When some motor designs do not fulfil geometrical constraints, a repair algorithm identify the violated constraint and tries if possible to change the motor design variables in order to fulfil them. However, this is done in a non-deterministic way by introducing a random factor in order to maintain some diversity among repair individuals.

6. Results

6.1 First optimization

A population of P=30 individuals and G=60 generations, with crossover probability p_c=0.9 and distribution index μ_c=20, mutation probability p_m=1/D (D=13 being the number of design variables) and distribution index μ_m=20, is here considered. The initial population is randomly generated in design variables bounds of Table 1(note that all the industrial design variables belong to these intervals, but that the industrial design has not been included on purpose in the initial population). The fitness $\mathbf{f}_{ref}$ of the industrial design $\mathbf{X}_{ref}$ is computed, and some normalization factors are introduced so that $\mathbf{f}_{ref}$

becomes equal to [0.5 0.5 0.5 0.5].

The evaluation of an individual objectives at a given motor speed takes 3 s on a 2 GHz processor laptop. The variable-speed simulation is carried at 30 different speeds, resulting in a total evaluation time of 90 s for one individual: the optimization therefore takes about two days to run. At fourth generation, all the individuals were feasible.

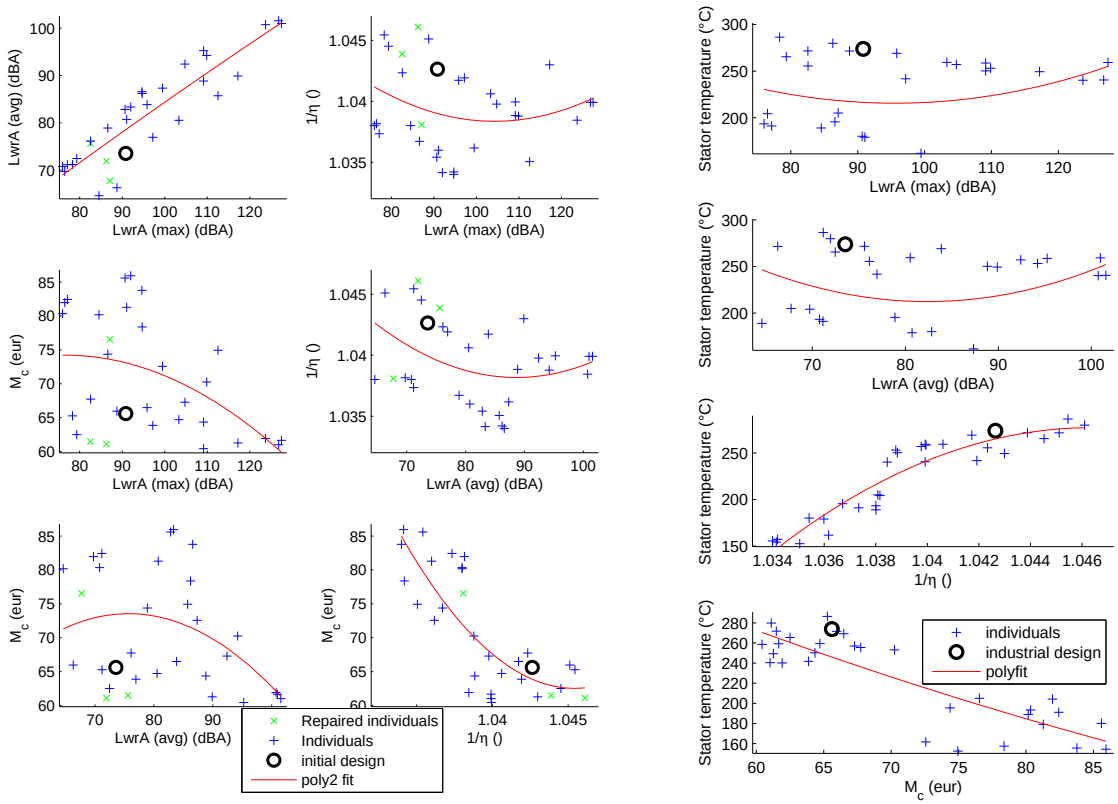

Figure 3: Left: final population (Pareto front) objectives 2-D projections. Right: individuals stator temperature in function of objectives.

When dealing with more than three objectives, it is impossible to visualize the whole Pareto front in a single figure. However, it is always possible to draw all its 3-D or 2-D projections. These 2D projections are shown in Fig. 3, where the industrial design has been marked, as well as the interpolated polynomial shape of the projected front.

The convexity of these curves are useful to identify the hardest trade-offs to make: for instance, a strong trade-off exists between efficiency and material cost, whereas average and maximum noise can clearly be minimized at the same time. The other projections show more scattered individuals, which means in particular that lowering magnetic noise does not necessarily lead to a higher material cost: indeed, a slight change of Z_r remain material cost unchanged, while it can significantly alter noise radiation.

In a same way, the evolution of stator mean temperature in function of the four objectives is drawn in Fig. 3 (rotor temperature case is similar): it can be seen that decreasing stator temperature increases motor efficiency, as it decreases stator resistance and consequently stator Joule losses. This figure also shows that the final population can be divided in two main groups: a first one with rather high temperature and low material cost, and a second one with low temperature and high material cost.

As an industrial design is known, it is of main interest to compare it with the current population. This comparison is drawn in Fig. 4, where the objective improvements are computed in percentage: no

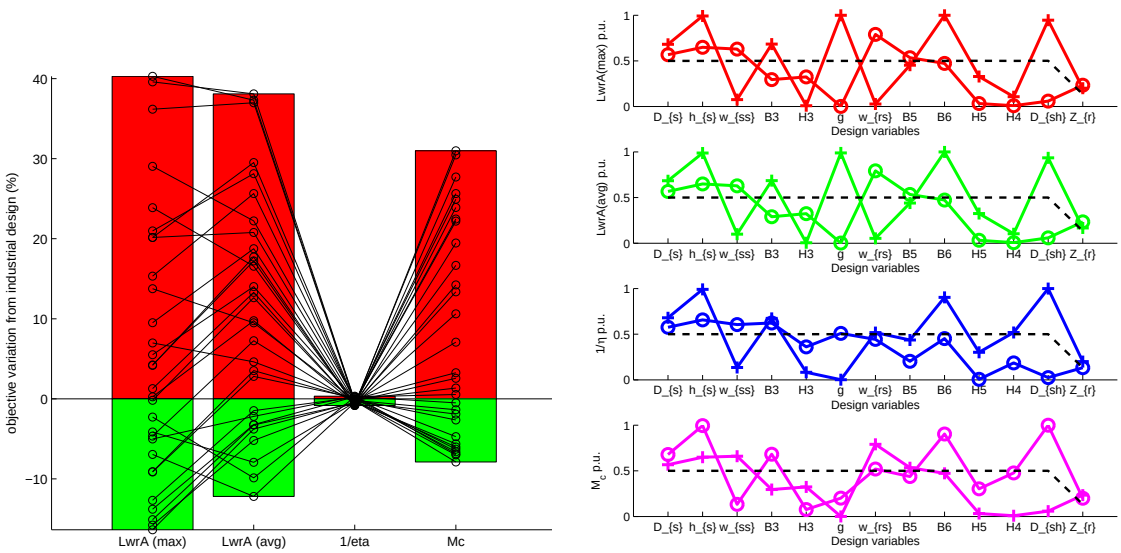

Figure 4: Left: final population improvements of industrial design objectives. Right: design variables representation of the eight individuals minimizing (+) or maximizing (0) each of the objectives.

individual improves all the objectives at the same time. For example a 10 % decrease in maximum noise can be reached, but either with an efficiency decrease or a material cost increase.

Fig. 4 shows the design variables value of the Pareto front extreme individuals, i.e. which either maximize or minimize one of the objectives. As predicted [12, 9], best noise objectives are reached with large air-gaps, high heights of yoke, and small stator and rotor slot openings. The stator core diameter has small influence on noise because the total diameter of the machine, including frame, is fixed during the optimization. The most efficient motor is of course reached with the lowest air-gap value, while the cheaper motor is obtained with the deepest slots and lowest height of yoke.

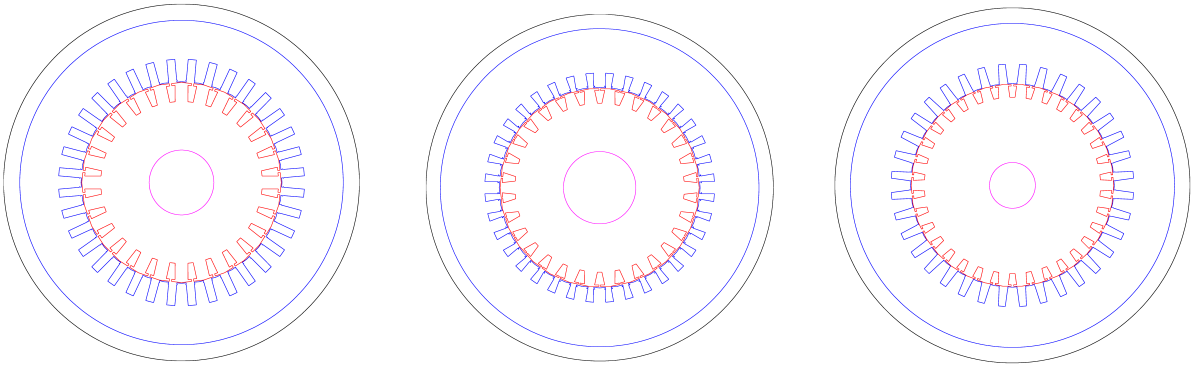

Industrial motor ($Z_r = 28$) Quietest motor($Z_r = 30$) Noisiest machine ($Z_r = 32$)

Figure 5: Motor sections of different individuals.

The geometry of the industrial design, as well as Pareto front individuals with the lowest and highest average noise, are represented in Fig. 5. The motor with $Z_r = 32$ is the noisiest: it creates a Maxwell force wave of order $Z_s - Z_r - 2p = 2$ which resonates near 1500 rpm with the ovalization mode of the stator, whose natural frequency is around 800 Hz.

6.2 Second optimization

As seen in previous section, none of the individuals improve all the objectives of the existing industrial design at the same time. Thus, a second optimization is run with exactly the same parameters, but with the additional constraint vector $\mathbf{f} - \mathbf{f}_{ref} \leq 0$.

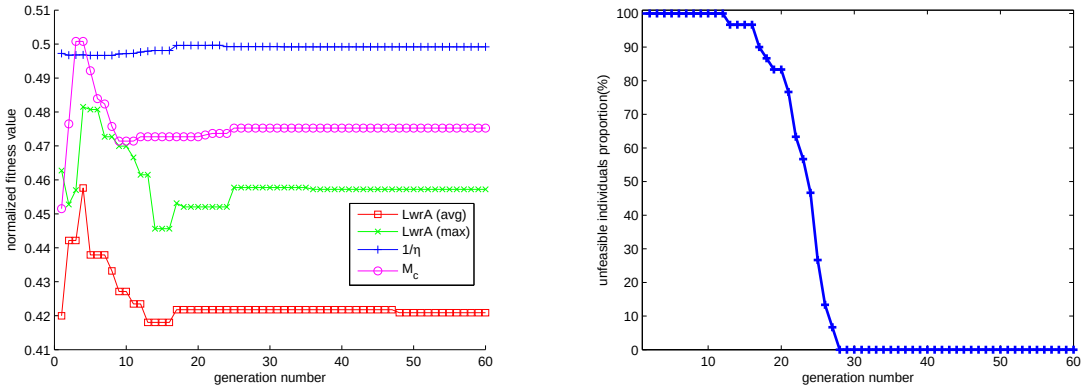

Figure 6: Left: evolution of best fitnesses during generations (normalized industrial design objectives are $\mathbf{f}_{ref}$=[0.5 0.5 0.5 0.5]). Right: evolution of unfeasible individuals amount during generations.

The evolution of population best fitnesses is presented in Fig. 6: at the beginning of the optimization, all the objectives are degraded in order to find feasible individuals. Once the whole population is feasible, best fitnesses do not improve very much.

The evolution of the number of feasible individuals among the current population is also presented in Fig. 6: current population is fully feasible after 28 generations. In the final population, all the individuals improve the first objective of the industrial design.

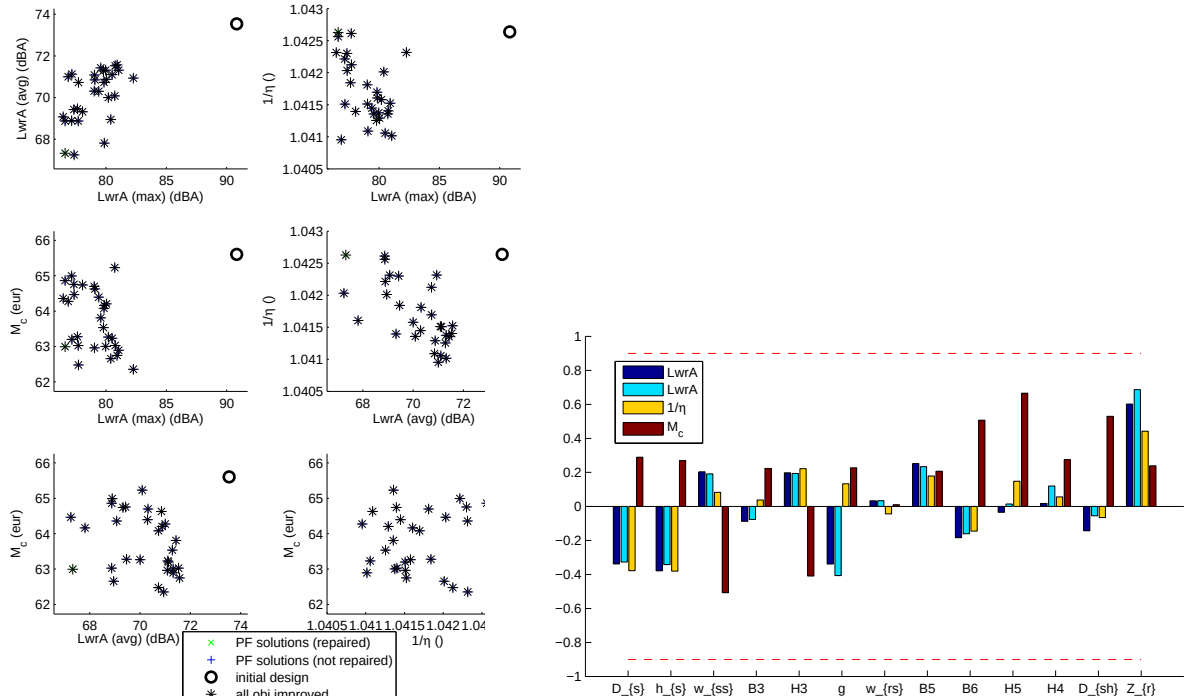

Figure 7: Left: final population (Pareto front) objectives 2-D projections. Right: correlation factors between design variables and objectives.

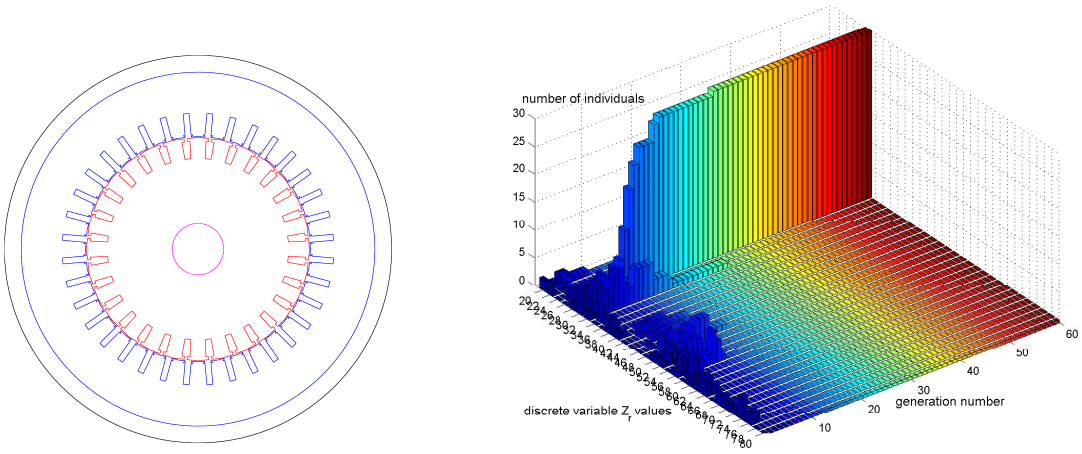

Figure 8: Left: an example of individual improving all the objectives of the industrial design. Right: evolution of Z_r discrete variable distribution in current population.

The Pareto front projections in Fig. 7 confirms that the industrial design is dominated by the whole population. As an example, the design presented in Fig. 8 has a maximum noise 15 % lower, an average noise 6 % lower, an efficiency 0.08 % higher and a material cost 4 % lower. Fig. 7 also shows a part of the correlation factors that were computed at the end of the optimization: all the generations design variables, objectives and constraints are used in order to calculate the correlation factors between one another. This is especially useful to quantify how the different objectives are linked one to another, and how design variables or constraints are linked to the objectives.

Fig. 8 also shows the evolution of the distribution of Z_r discrete variable among the population during generations: although the numbers of teeth were very different in the initial population, and the industrial design with $Z_r = 28$ is not included, the individuals have all converged towards $Z_r = 28$. The final Pareto front is not very well-spread in the objectives space, as indicated by the deviation factor Δ [10] which here equals to 5.10^{-5} against 18.47 in the first optimization.

7. Conclusions

A multidisciplinary analytical model of the squirrel-cage induction motor, including electromagnetic, thermal, mechanical and acoustic parts, has been built and validated with FEM and/or tests. It has been coupled to a constrained mixed-variable multi-objective optimization algorithm, and new designs improving at the same time the industrial motor audible magnetic noise, efficiency and material cost have been found.

Future work aims at including harmonic losses due to pulse-width modulation supply in the model, and coupling the optimization algorithm to a clustering method in order to identify motor lines in the Pareto front.

References

[1] P. Timar, *Noise and vibration of electrical machines.* Elsever, 1989.

[2] H. Jordan, *Electric motor silencer - formation and elimination of the noises in the electric motors.* W. Giradet-Essen editor, 1950.

[3] S. J. Yang, *Low noise electrical motors.* Oxford: Clarendon Press, 1981.

[4] H. Huang, E. Fuchs, and Z. Zak, "Optimization of single-phase induction motor design," *IEEE Trans. on Energy Conversion*, vol. 3, no. 2, June 1988.

[5] G. Liuzzi, S. Lucidi, F. Parasiliti, and M. Villani, "Multiobjective optimization techniques for the design of induction motors," *IEEE Trans. on Magnetics*, vol. 39, no. 3, May 2003.

[6] M. Poloujadoff, E. Christaki, and C. Bergniann, "Univariant search: An opportunity to identify and solve conflict problems in optimization," *IEEE Trans. on Energy Conversion*, vol. 9, no. 4, Dec. 1994.

[7] C. Singh and D. Sarkar, "Practical considerations in the optimisation of induction motor design," *IEE Proceedings*, vol. 139, no. 4, July 1992.

[8] A. H. Amor, P. Timar, and M. Poloujadoff, "Induction squirrel cage machine design with minimization of electromagnetic noise," *IEEE Transactions on Energy Conversion*, vol. 10, no. 4, Dec. 1995.

[9] J. L. Besnerais, V. Lanfranchi, M. Hecquet, P. Brochet, and G. Friedrich, "Acoustic noise of electromagnetic origin in a fractional-slot induction machine," *COMPEL*, vol. 27, no. 5, Feb. 2008.

[10] K. Deb, A. Pratap, S. Agarwal, and T. Meyarivan, "A fast and elitist multiobjective genetic algorithm: NSGA-II," *IEEE Trans. on Evolutionary Computation*, vol. 6, no. 2, Apr. 2002.

[11] M. Liwschitz, *Calcul des machines électriques.* Spes Lausanne, 1967.

[12] J. L. Besnerais, A. Fasquelle, M. Hecquet, V. Lanfranchi, P. Brochet, and A. Randria, "A fast noise-predictive multiphysical model of the PWM-controlled induction machine," in *Proc. of the International Conference on Electrical Machines (ICEM'06)*, Chania, Greece, July 2006.

[13] A. Fasquelle, A. Ansel, S. Brisset, M. Hecquet, P. Brochet, and A. Randria, "Iron losses distribution in a railway traction induction motor," in *Proc. of the International Conference on Electrical Machines (ICEM'06)*, Chania, Greece, July 2006.

[14] A. Fasquelle, D. Saury, S. Harmand, and A. Randria, "Numerical study of convective heat transfer in end region of enclosed induction motor of railway traction," *IJEET International Journal of Electrical Engineering in Transportation*, Dec. 2006.

[15] P. Alger, *Induction machines : their behaviour and uses.* Gordon and Breach Science Publishers, 1970.

[16] A. Hubert, "Contribution l'étude des bruits acoustiques générés lors de l'association machines électriques - convertisseurs statiques de puissances - application la machine asynchrone," Ph.D. dissertation, Université des Technologies de Compiègne, France, Dec. 2000.

[17] J. L. Besnerais, V. Lanfranchi, M. Hecquet, and P. Brochet, "Calcul du bruit acoustique d'une machine asynchrone a pas fractionnaire," in *Proceeding of EF'07*, Sept. 2007.

[18] A. Ait-Hammouda, M. Hecquet, M. Goueygou, and P. Brochet, "Prediction of the electromagnetic noise of an asynchronous machine using experimental designs," *Mathematics and Computers in Simulation*, vol. 71, no. 4, June 2006.

[19] J. L. Besnerais, V. Lanfranchi, M. Hecquet, and P. Brochet, "Multi-objective optimization of the induction machine with minimization of audible electromagnetic noise," *European Physics Journal - Applied Physics*, vol. 39, no. 2, Aug. 2007.

[20] ——, "Multi-objective optimization of induction machines including mixed variables and noise minimization," *IEEE Trans. on Mag.*, vol. 44, no. 4, Apr. 2008.

[21] K. Deb, *Multi-objective optimization using evolutionary algorithms.* John Wiley & Sons, 2002.

[22] M. Mohan, K. Deb, and S. Mishra, "A fast multi-objective evolutionary algorithm for finding well-spread Pareto-optimal solutions," Kanpur Genetic Algorithms Laboratory (KanGAL), Tech. Rep., 2003.